

Initial operation of perpendicular line-of-sight compact neutron emission spectrometer in the large helical device

メタデータ	言語: eng 出版者: 公開日: 2022-09-14 キーワード (Ja): キーワード (En): 作成者: SANGAROON, Siriyaporn, OGAWA, Kunihiro, ISOBE, Mitsutaka メールアドレス: 所属:
URL	http://hdl.handle.net/10655/00013477

This work is licensed under a Creative Commons Attribution 3.0 International License.



Initial operation of perpendicular line-of-sight compact neutron emission spectrometer in the Large Helical Device

S. Sangaroon,^{1,a),b)} K. Ogawa,^{2,3,b)} and M. Isobe,^{2,3,b)}

¹*Department of Physics, Faculty of Science, Mahasarakham University, Maha Sarakham, 44150, Thailand.*

²*National Institute for Fusion Science, National Institutes of Natural Sciences, Toki 509-5292, Japan*

³*The Graduate University for Advanced Studies, SOKENDAI, Toki 509-5292, Japan*

(Presented XXXXX; received XXXXX; accepted XXXXX; published online XXXXX)

The perpendicular line-of-sight compact neutron emission spectrometer (perpendicular CNES) was newly installed to understand the helically-trapped fast-ion behavior through deuterium-deuterium (D-D) neutron energy spectrum measurement in Large Helical Device (LHD). The energy calibration of the EJ-301 liquid scintillation detector system for perpendicular CNES was performed in an accelerator-based D-D neutron source. We installed two EJ-301 liquid scintillation detectors, which view the LHD plasma vertically from the lower side through the multichannel collimator. The D-D neutron energy spectrum was measured in a deuterium perpendicular-neutral-beam-heated deuterium plasma. By the derivative unfolding technique, it was found that the D-D neutron energy spectrum had a double humped shape with peaks at ~ 2.33 MeV and ~ 2.65 MeV. D-D neutron energy spectrum was calculated based on the fast ion distribution function using guiding center orbit-following models considering the detector's energy resolution. The calculated peak energies in the D-D neutron energy spectrum almost match the experiment. In addition, the feasibility study toward the measurement of the energy distribution of ion-cyclotron-range-of-frequency-wave-accelerated beam ion was performed.

I. INTRODUCTION

In present-day fusion plasma experiments, plasmas are mainly heated by fast ions generated by neutral beam injection (NBI) and/or ion cyclotron range of frequency (ICRF) wave. Understanding the fast-ion's behavior is therefore crucial for achieving higher-performance plasmas.¹ At the same time, the pressure of fast ions can be a free energy source to excite fast-ion-driven magnetohydrodynamic (MHD) instabilities which might cause the enhanced transport of fast ions.

The comprehensive set of neutron diagnostics providing fast-ion information has been working in the Large Helical Device (LHD) since March 2017.²⁻⁵ Confinement of passing and helically-trapped beam ions in MHD quiescent plasmas has been studied by decay time of total neutron emission rate S_n in short pulse deuterium NBI experiments using the neutron flux monitor (NFM).⁶ It was reported that the confinement of beam ions becomes better with inward shift of the magnetic axis.⁷ For the fast-ion-driven MHD instability study, radial transport of helically-trapped beam ions due to fast-ion-driven MHD instability has been visualized^{8,9} using vertical neutron cameras.^{10,11} For a deeper understanding of the classical confinement of fast ions and the excitation mechanism of the fast-ion-

driven MHD instabilities, information on the fast ion energy distribution is additionally required.

To understand the energy distribution of fast ions, we have been developing neutron energy spectrometers in LHD.¹² Since 2020, the tangential line-of-sight compact neutron emission spectrometer (tangential CNES) has been operated.¹³ Significant Doppler shift in deuterium-deuterium (D-D) neutron energy reflecting the energy distribution of passing beam ions injected by negative-ion-source-based tangential NBI (N-NB) has been reported.^{14,15} In 2021, to understand helically-trapped beam ion energy distribution, a new perpendicular line-of-sight CNES (perpendicular CNES) was installed. In this paper, we report the detail and initial operation of perpendicular CNES. The conventional liquid organic scintillator is used for the perpendicular CNES due to its relatively fast decay time (\sim ns), thus, the perpendicular CNES can operate during the high S_n . Liquid organic scintillation detector become important in fusion device for fast neutron spectroscopy due to their relatively high light output, good detection efficiency, fast decay time and excellent n/γ pulse shape discrimination capabilities.^{16,17} Together with the suitable unfolding technique, the CNES base on liquid scintillator can provide the high-resolution neutron spectrometer.

II. THE CHARACTERIZATION OF EJ-301 LIQUID SCINTILLATION DETECTOR SYSTEM

The energy calibration of the EJ-301 liquid scintillation detector system used for perpendicular CNES was performed using an accelerator-based neutron source in the fast neutron laboratory (FNL) of Tohoku University¹⁸

^{a)} Author to whom correspondence should be addressed. Electronic mail: siriyaporn.s@msu.ac.th.

^{b)} S. Sangaroon, K. Ogawa, and M. Isobe contributed equally to this work.

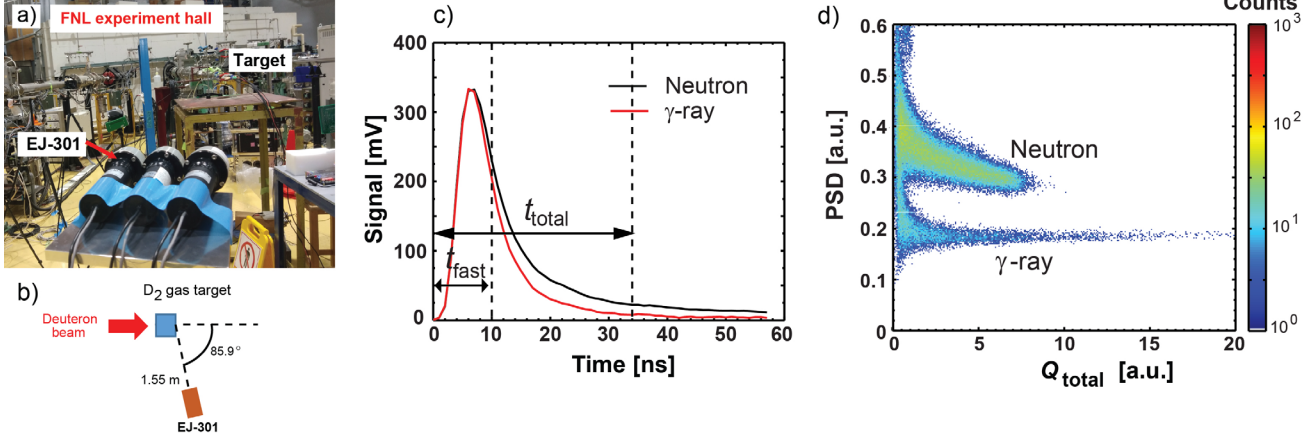


FIG. 1. a) Arrangement of FNL experiment. b) Schematic top view of FNL D-D experiment where the detector is placed at 85.9 deg. from the beam axis. c) The typical neutron and γ -ray induced signal measured by EJ-301 scintillation detector. d) Two-dimensional PSD plot.

(Fig. 1a). The system is composed of an EJ-301 liquid scintillation detector and fast digital data acquisition (DAQ). The EJ-301 scintillator¹⁹, with 1-inch in diameter and in height, is directly coupled to a 1-inch photomultiplier tube (PMT) (H10580-100-01, Hamamatsu Photonics K.K.).²⁰ The anode signal of the detector is fed into the fast DAQ (APV8102-14MWPSAGb, Techno AP Corp.).²¹ The deuteron beam with 1.5 MeV, 2.0 MeV, and 3.0 MeV was respectively injected into the D_2 gas target to obtain a rather monoenergetic D-D neutron. The EJ-301 scintillation detector was placed at 15.5 deg., 60.8 deg., and 85.9 deg. from the beam axis (Fig. 1b), where the D-D neutron energy peak at the detector position was expected to be ~ 2.5 MeV to ~ 5.5 MeV. Pulse shape discrimination PSD = $(Q_{\text{total}} - Q_{\text{fast}})/Q_{\text{total}}$, where Q_{total} is an integrated signal in t_{total} of 34 ns and Q_{fast} is an integrated signal in t_{fast} of 10 ns, is used for discriminating fast-neutron and γ -ray (Fig. 1c and 1d). In this neutron energy range, neutron-proton elastic scattering mainly occurs with the EJ-301 scintillator. The

relation between the recoiled proton energy E_p and Q_{total} : E_p [MeV] = $0.22 \times Q_{\text{total}} + 0.98$ was obtained using maximum Q_{total} and expected D-D neutron energy peak at the detector position.

The unfolding of the D-D neutron energy spectrum $\phi(E_n)$ from E_p distribution was performed using the experimental result in the 1.5 MeV deuteron beam and 85.9 deg. detector position case. The derivative unfolding²² using $\phi(E_n) = \frac{-E_p}{TnV\sigma(E_p)} [y'(x)\{gL'(E_p)\}^2 + y(x)gL''(E_p)]$ was conducted. Here, T , n , V , σ , $y(x)$, g , $L(E_p)$, $'$, and $''$ represent the time duration, the density of hydrogen atom, the detector volume, the neutron-proton elastic scattering cross section, Q_{total} histogram, the PMT gain 6.6×10^5 , light output as a function of the recoil particle energy²³, the first derivative, and the second derivative, respectively. Note that the detection efficiency is not considered in this calculation. The black line in Fig. 2 shows the unfolded $\phi(E_n)$. The energy resolution of the EJ-301 liquid scintillation detector system $R(E_n)$ was evaluated by comparing experimentally obtained $\phi(E_n)$ and the calculated neutron flux $\Gamma(E_n)$ at the detector position. Here, the deuteron beam's energy spectrum in the D_2 gas target and the neutron transport in FNL experiment hall were estimated by TRIM code²⁴ and MCNP code²⁵, respectively. Here, $R(E_n) = \sqrt{a^2 + b^2/E_n + c^2/E_n^2}$ was assumed according to Ref. 26. Coefficients $a = 0.046$, $b = 0.069$, and $c = 0.009$ were determined through iterations that $\Gamma(E_n) \times R(E_n)$ matched experimentally obtained $\phi(E_n)$ (Fig. 2). It is worth noting that $R(E_n)$ was gradually changed from 7% to 6% in E_n from 1.8 MeV to 3.2 MeV. The discrepancy of neutron energy spectrum at E_n below ~ 2.4 MeV might be caused by the scattered neutron effect.

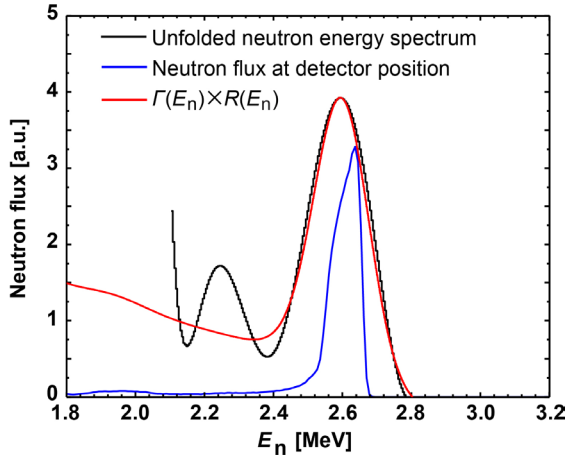


FIG. 2. Comparison of unfolded neutron energy spectrum, neutron flux at detector position, and calculated neutron energy spectrum when the detector's energy resolution is taken into account when deuteron beam with an energy of 1.5 MeV was injected into the D_2 gas target and the detector is placed at 85.9 deg. from the beam axis.

III. MEASUREMENT OF D-D NEUTRON ENERGY SPECTRUM IN P-NB HEATED DEUTERIUM PLASMA IN LHD

We installed the EJ-301 liquid scintillation detector system in LHD. Two EJ-301 scintillation detectors are placed below the multichannel collimator and view the plasma vertically from the lower side at the 1.5-L port (Fig.

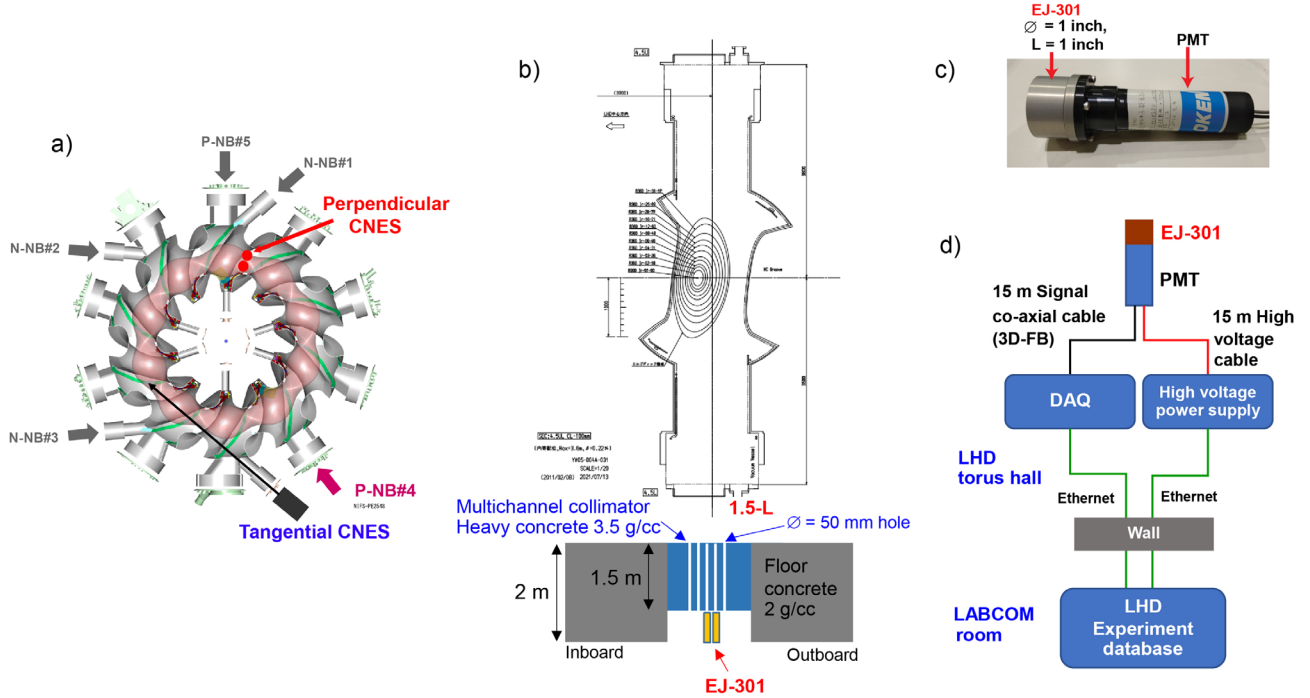


FIG. 3. a) A schematic top view of LHD, P-NB#4, and CNESs. b) A schematic drawing of the LHD cut view at 1.5-L port and the perpendicular CNES. c) EJ-301 liquid scintillation detector. d) Electronics schematic of perpendicular CNES.

3). The radial position (R) of the detectors are 3.725 m and 3.875 m, respectively. The detectors are biased with a high voltage (APV3304, Techno AP Corp.).²⁷ The digitized data obtained by DAQ is transferred to the LHD experiment database via 1 Gbps ethernet.

Measurement of D-D neutron energy spectrum by perpendicular CNES was conducted in P-NB heated deuterium plasma discharge #173908 (Fig. 4). In the

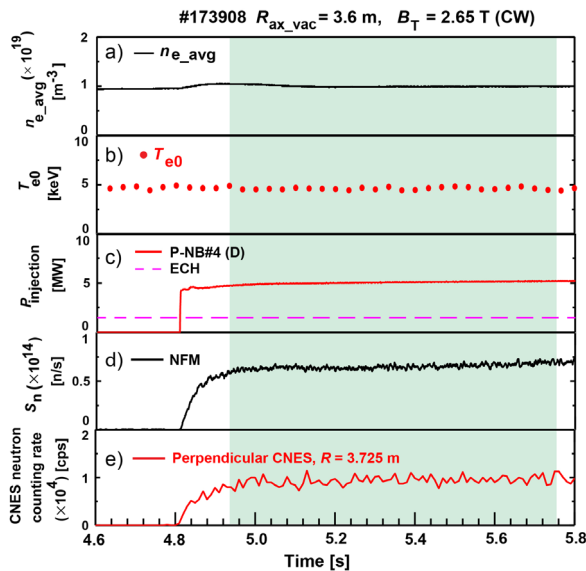


FIG. 4. Time evolution of deuterium plasma discharge #173908 performed in LHD. a) Line-averaged electron density n_{e_avg} . b) Central electron temperature T_{e0} . c) P-NB#4 is injected during selected time. d) S_n measured by NFM. e) Neutron counting rate measured by perpendicular CNES at R of 3.275 m. Time interval between 4.93 s to 5.75 s is selected (green-shaded).

experiment, the magnetic axis position in vacuum R_{ax_vac} was 3.60 m and toroidal magnetic field strength B_T was set to be 2.65 T with clockwise (CW) directions viewed from the top. P-NB#4 was injected continuously with the energy of ~ 50 keV and power of ~ 5 MW. The neutron counting rate measured by the perpendicular CNES ($R = 3.725$ m) shows the same trend as S_n . Here, neutron pulses are discriminated using the PSD method. A time interval from 4.93 s to 5.75 s was selected for D-D neutron energy spectrum analysis, where the bulk plasma parameters were almost unchanged. We unfolded $\phi(E_n)$ from Q_{total} histogram measured by the perpendicular CNES (Fig. 5a) using the derivative unfolding method. It was shown that the unfolded $\phi(E_n)$ has a double humped shape, with the peaks at ~ 2.33 MeV and ~ 2.65 MeV (Fig. 5b). Two peaks might be corresponding to Larmor motion of perpendicular beam ion.²⁸

IV. COMPARISON OF D-D NEUTRON ENERGY SPECTRUM IN EXPERIMENT AND CALCULATION

The numerical simulation based on the orbit following model was performed to understand the D-D neutron energy spectrum measured in the P-NB heated plasma. The three-dimensional MHD equilibrium was reconstructed by VMEC2000 code²⁹ using the pressure profile given by TSMAP.³⁰ The HFREYA code^{31,32} was utilized to calculate the birth position of the beam ions generated by P-NB. The guiding-center orbits of the 10^5 P-NB ions in the Boozer coordinates were followed within 1 s by the DELTA5D code.³³ D-D neutron energy spectrum expected to be obtained by perpendicular CNES is calculated with

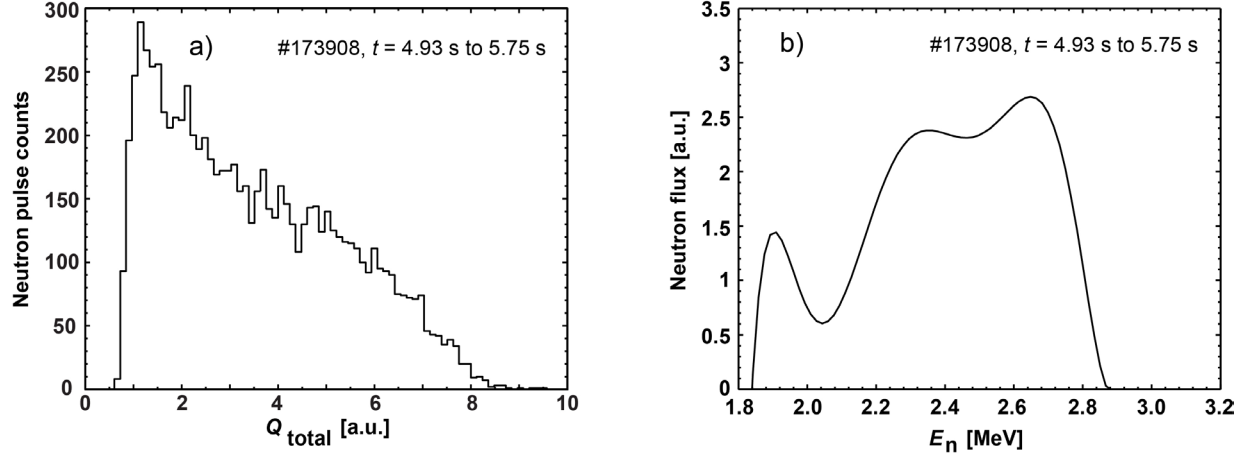


FIG. 5. a) histogram of the Q_{total} and b) unfolded D-D neutron energy spectrum measured by perpendicular CNES, when the detector is at $R = 3.725$ m, performed in P-NB heated deuterium plasma discharge #173908.

considering the beam ion energy distribution, Larmor phase, and detector's energy resolution (Fig. 6).

Beam ion energy distribution of deuterium plasma discharge #173908 at time $t = 5.3$ s integrated over perpendicular CNES sightline obtained by DELTA5D code is shown in Fig. 7a. Figure 7b shows the calculated D-D neutron energy spectrum obtained by perpendicular CNES. The calculated $\phi(E_n)$ has a double humped shape with the peaks at ~ 2.33 MeV and ~ 2.65 MeV. Although the relative height of the two peaks shows different characters, the peak energies agree with the experiment. The discrepancy in relative height of two peaks and understanding of a peak at 1.9 MeV obtained in the experiment are our future work.

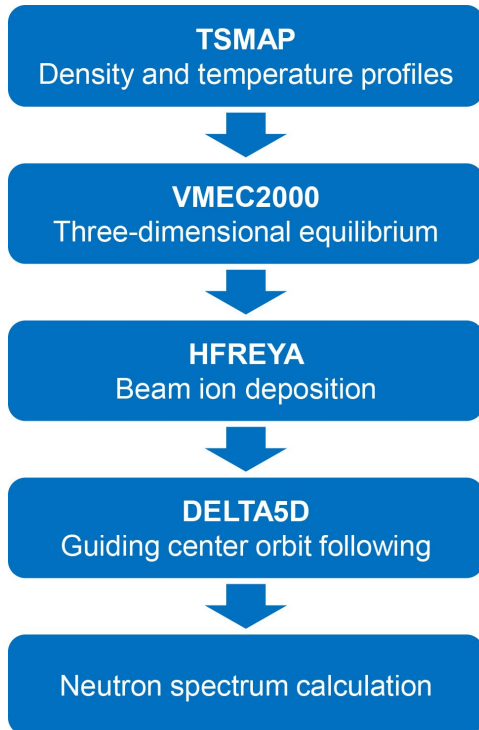


FIG. 6. Flowchart of the setup for D-D neutron energy spectrum calculations.

Furthermore, the affect between two sightlines of perpendicular CNES on the D-D neutron energy spectra will be discussed in the future work.

V. FEASIBILITY STUDY TOWARD D-D NEUTRON ENERGY SPECTRUM MEASUREMENT IN ICRF WAVE AND NBI HEATED PLASMA

A feasibility study toward D-D neutron energy spectrum measurement in ICRF-wave- and NBI-heated deuterium plasmas was performed. In such experiments, beam ions can be accelerated by the ICRF wave. The measurement of the energy distribution of the ions through the D-D neutron energy spectrum could contribute to understanding the acceleration process. In this study, we used a simple model that the test particles assumed to have the beam ion slowing down distribution, and we changed the initial test particle energy from 80 keV to 1000 keV. Test particle energy distributions integrated over perpendicular CNES sightline calculated by DELTA5D code for each case are shown in Fig. 8a. Figure 8b shows the D-D neutron energy spectrum obtained by perpendicular CNES. The neutron energy spectrum expected to be obtained by perpendicular CNES shows that the peak locations shifted according to the test particle energy. The perpendicular CNES can be a candidate diagnostic for studying beam ion acceleration by ICRF wave.

VI. SUMMARY

Perpendicular line-of-sight CNES was newly installed to understand the behaviour of helically-trapped fast ions in the LHD. The energy calibration of the EJ-301 liquid scintillation detector system used for the perpendicular CNES was performed in an accelerator-based neutron source. We measured the D-D neutron energy spectrum by the perpendicular CNES in a deuterium P-NB heated LHD plasma. It was shown that the D-D neutron energy spectrum has a double humped shape with peaks at ~ 2.33 MeV and ~ 2.65 MeV using the derivative unfolding method. The neutron energy spectrum calculation based on the orbit

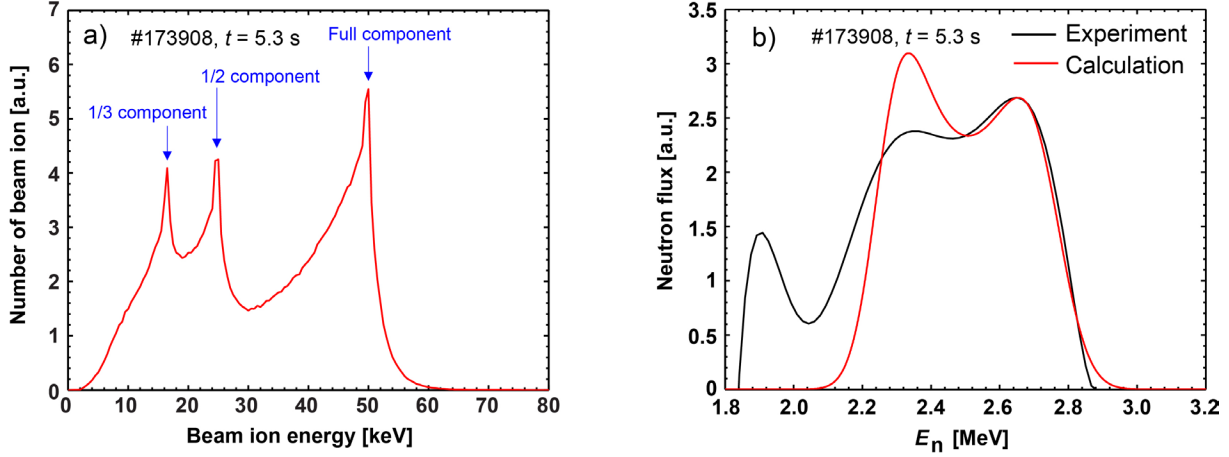


FIG. 7. a) Beam ion energy distribution integrated over perpendicular CNES sightline and b) D-D neutron energy spectrum obtained by perpendicular CNES, when the detector is at $R = 3.725$ m, in the experiment and calculation.

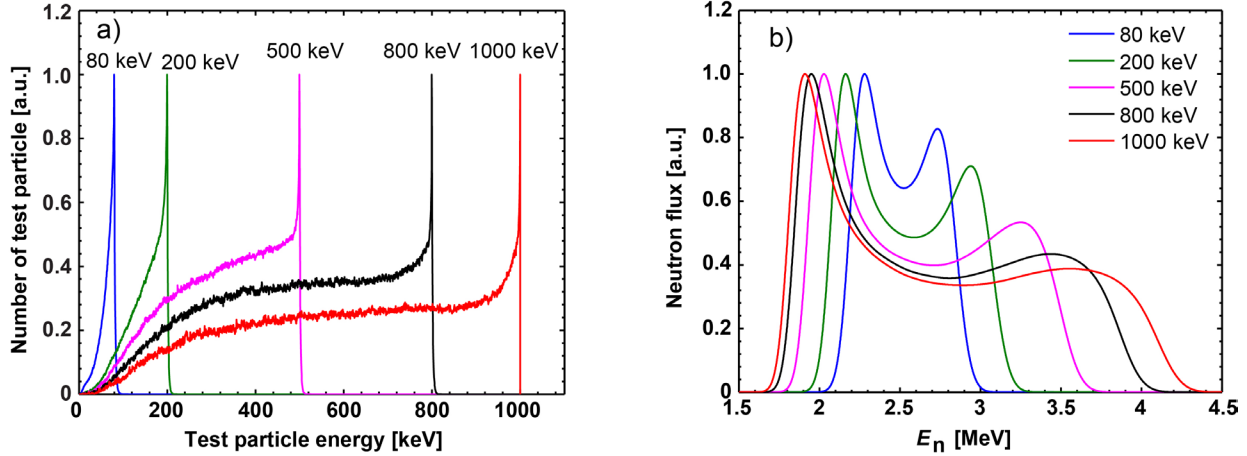


FIG. 8. a) Test particle energy distribution integrated over perpendicular CNES sightline and b) D-D neutron energy spectrum expected to be obtained by perpendicular CNES when the detector is at $R = 3.725$ m.

following model was performed. The peak positions of the calculated neutron energy spectrum agree with the experiment. A feasibility study toward an understanding of beam ion acceleration by ICRF wave was performed. The perpendicular CNES might contribute to understanding the beam ion acceleration process.

DATA AVAILABILITY STATEMENT

The LHD data can be accessed from the LHD data repository at https://www-lhd.nifs.ac.jp/pub/Repository_en.html.

ACKNOWLEDGMENTS

This research was supported by NIFS Collaboration Research programs (KOA037), by the NINS program of Promoting Research, by Networking among Institutions (Grant Number 01411702), by Thailand Institute of Nuclear Technology (TINT), and by NSRF via the Program Management Unit for Human Resources & Institutional Development, Research and Innovation (Grant Number B05F640224). We are pleased to acknowledge the assistance of the LHD Experiment Group.

REFERENCES

- ¹A. Fasoli et al., Nuclear Fusion **47**, S264 (2007).
- ²M. Isobe et al., IEEE Trans. Plasma Sci. **46**, 2050 (2018).
- ³M. Isobe et al., Nucl. Fusion **58**, 082004 (2018).
- ⁴K. Ogawa et al., Nucl. Fusion **59**, 076017 (2019).
- ⁵K. Ogawa et al., Plasma Fusion Res. **16**, 1102023 (2021).
- ⁶M. Isobe et al., Rev. Sci. Instrum. **85**, 11E114, (2014).
- ⁷H. Nuga et al., J. Plasma Phys. **86**, 815860306 (2020).
- ⁸K. Ogawa et al., Nucl. Fusion **58**, 044001 (2018).
- ⁹K. Ogawa et al., Nucl. Fusion **60**, 112011 (2020).
- ¹⁰K. Ogawa et al., Rev. Sci. Instrum. **89**, 113509 (2018).
- ¹¹S. Sangaroon et al., Rev. Sci. Instrum. **91**, 083505 (2020).
- ¹²M. Isobe et al., Plasma Fusion Res. **17**, 2402008 (2022).
- ¹³M. Isobe et al., J. Instrum. **17**, C03036 (2022).
- ¹⁴S. Sangaroon et al., J. Instrum. **16**, C12025 (2021).
- ¹⁵S. Sangaroon et al., AAPPS Bulletin **32**, 5 (2022).
- ¹⁶A. Zimba et al., Review of Scientific Instruments **75**, 3553 (2004).
- ¹⁷F. Belli et al., IEEE Tran. Nucl. Sci. **59**, 2512 (2012).
- ¹⁸M. Baba et al., Nucl. Instrum. Methods Phys. A **376**, 115-123 (1996).

¹⁹See <https://eljentechnology.com/products/liquid-scintillators/ej-301-ej-309> for the specification of the EJ-301 scintillator.

²⁰See https://www.hamamatsu.com/resources/pdf/etd/High_ener_gy_PMT_TPMZ0003E.pdf for H10580-100-01 for the photomultiplier tube.

²¹See http://www.techno-ap.com/img/APV8102-14MWPSAGb_e.pdf for DAQ system.

²²D. R. Slaughter et al., Nucl. Instrum. Methods **198**, 349–355 (1982).

²³V. V. Verbinski et al., Nucl. Instrum. Methods **65**, 8–25 (1968).

²⁴See <http://www.srim.org/> for TRIM code.

²⁵D. B. Pelowitz, LA-CP-13-00634, Los Alamos National Laboratory (2013).

²⁶G. Dietze and H. Klein Nucl. Instrum. Methods **193**, 549–556 (1982).

²⁷See http://www.techno-ap.com/img/APV3304_e.pdf for the APV3304 high voltage power supply board.

²⁸J. Eriksson et al., Plasma Phys. Control. Fusion **55**, 015008 (2013).

²⁹S. P. Hirshman and O. Betancourt J. Comput. Phys. **96**, 99 (1991).

³⁰C. Suzuki et al., Plasma Phys. Control. Fusion **55**, 014016 (2013)

³¹S. Murakami et al., Trans. Fusion Technol. **27**, 256 (1995).

³²P. Vincenzi et al., Plasma Phys. Control. Fusion **58**, 125008 (2016).

³³D. A. Spong et al., Phys. Plasmas **18**, 056109 (2011).